

# Measurement of the timelike neutron and proton form factors at VEPP-2000

A.A.Korol<sup>1,2</sup> (for the CMD-3 and SND Collaborations)

<sup>1</sup> Budker Institute of Nuclear Physics, Novosibirsk, Russia

<sup>2</sup> Novosibirsk State University, Novosibirsk, Russia

**Abstract:** We present the results of the study of the  $e^+e^- \rightarrow n\bar{n}$  and  $e^+e^- \rightarrow p\bar{p}$  reactions in the energy range from the nucleons production threshold up to 2 GeV. The measurements have been performed at the VEPP-2000  $e^+e^-$  collider with the SND and CMD-3 detectors using the events collected during the data taking runs of 2011 and 2012. We also discuss here obtained electromagnetic form factors of nucleons and future plans of these results improvement.

**Key words:** proton, neutron, electromagnetic form factor,  $e^+e^-$  annihilation, SND, CMD-3

**PACS:** 13.40.Gp,13.60.Rj,13.66.Bc,14.20.Dh

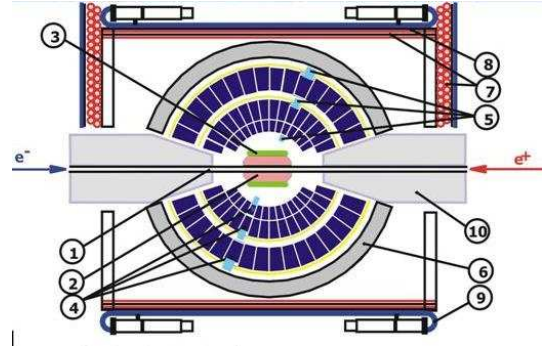
## 1 Introduction

Electromagnetic interaction of the nucleons (neutrons and protons) can be described with two complex functions of transferred momentum, the electric form factor  $G_E(s)$  and the magnetic form factor  $G_M(s)$ . In the timelike region above nucleons production threshold ( $s > 4M_N^2$ ) this functions can be partially extracted from the total cross section and the angle distribution in the annihilation processes  $e^+e^- \rightarrow p\bar{p}$  and  $e^+e^- \rightarrow n\bar{n}$ .

The early results were obtained by the Babar [5] and PS170 [6] experiments for protons and in the FENICE [7] experiment for neutrons. In this talk we review the results from the CMD-3 and SND detectors for the process  $e^+e^- \rightarrow p\bar{p}$ , and the result from the SND detector for process  $e^+e^- \rightarrow n\bar{n}$ . The data were collected at the VEPP-2000 collider [1] during the data taking runs in 2011 and 2012 at the center of mass energy range 1.8 to 2.0 GeV. The collider allows to study  $e^+e^-$  collisions at the center of mass energy range 0.3 to 2.0 GeV with the luminosity in the studied region ( $\sim 1.8\text{GeV}$ )  $L \sim 0.7 \cdot 10^{31} \text{cm}^{-2} \text{sec}^{-1}$  and the energy spread  $\delta_E \sim 0.6\text{MeV}$ . The detectors are located in the opposite sides of the VEPP-2000 collider. The data are being collected in parallel.

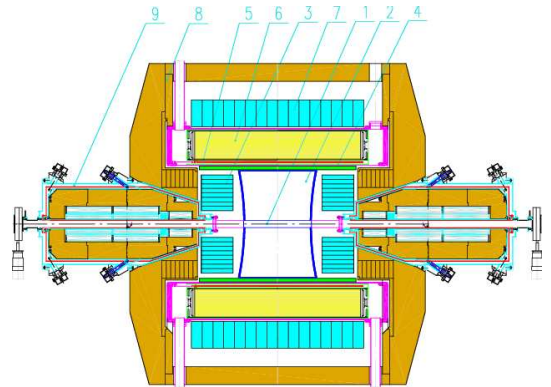
The SND ([2], Fig.1.) detector includes the drift chamber, the three layer electromagnetic (EMC) NaI(Tl) calorimeter and muon system.

Fig. 1. The SND layout (1 - beam pipe, 2 - tracking system, 3 - aerogel cherenkov counter, 4 - NaI(Tl) crystals, 5 - phototriods, 6 - iron muons absorber, 7-9 - muon system, 10 - VEPP-2000 solenoids).



The CMD-3 detector ([3], Fig.2) includes the drift chamber in the 1.3T magnetic field, EMC calorimeter consisting of BGO endcap and two barrel layers, LXe and CsI. It also includes the muon system.

Fig. 2. CMD-3 layout(1 - vacuum chamber, 2 - drift chamber, 3 - BGO calorimeter, 4 - Z-chamber, 5 - SC solenoid, 6 - LXe calorimeter, 7 - CsI calorimeter, 8 - yoke, 9 - VEPP-2000 solenoids).



The integrated luminosity collected in the region of

Received 30 Nov. 2015

1) E-mail: A.A.Korol@inp.nsk.su

interest is  $\sim 8.7\text{pb}^{-1}$  and summarized in Table.1

Table 1. The integrated luminosity.

Experiment	IL, $pb^{-1}$	IL( $\sqrt{s} > 1.88\text{GeV}$ ), $pb^{-1}$
12.2010-06.2011	25	3.8
01.2012-04.2012	17	4.9
Total	43	8.7

The differential cross section of the process  $e^+e^- \rightarrow N\bar{N}$  can be expressed as a function of transferred momentum squared ( $s$ ) and polar angle ( $\theta$ ):

$$\frac{d\sigma(s)}{d\Omega} = \frac{\alpha^2\beta C}{4s} \left( |G_M(s)|^2 (1 + \cos^2\theta) + \frac{4M_N^2}{s} |G_E(s)|^2 \sin^2\theta \right) \quad (1)$$

here  $C$  is the Coulomb factor [4] taking values  $C=1$  for neutron and  $C \approx \frac{\pi\alpha}{\beta}/(1-e^{-\frac{\pi\alpha}{\beta}})$  for proton,  $M_N$  is the nucleon mass,  $G_M(s)$  and  $G_E(s)$  are electric and magnetic form factors.

The full cross section then can be written as:

$$\sigma(s) = \frac{4\pi\alpha^2\beta C}{3s} \left( |G_M(s)|^2 + \frac{2M_N^2}{s} |G_E(s)|^2 \right) \quad (2)$$

It is convenient to use also “effective form factor” for comparison of the results from the different experiments:

$$F(s) = \frac{|G_M(s)|^2 + \frac{2M_N^2}{s} |G_E(s)|^2}{1 + \frac{2M_N^2}{s}} \quad (3)$$

The measured event distribution from  $\cos\theta$  can be used to obtain the ratio of electrical and magnetic form factors  $\frac{G_E(s)}{G_M(s)}$ .

## 2 CMD3 and SND $p\bar{p}$ measurements

The selection procedure of  $p\bar{p}$  events depends on the proton energy. Close to the kinematic threshold both protons and antiprotons stop in the beam pipe material with loss of the proton, while the antiproton gives an annihilation star. For the higher proton energy both the proton and the antiproton cross drift chamber, giving high dE/dX tracks. Then antiproton gives annihilation star in the outer wall of the drift chamber.

The main criteria to select  $p\bar{p}$  events at CMD-3 and  $E_{beam} < 950$  MeV (near the threshold), are the following[8]: 4 or more tracks with common vertex found in the beam pipe material; no tracks with energy deposition in calorimeter higher than 400 MeV. At  $E_{beam} \geq 950$  MeV two opposite-charge collinear central tracks in DC are required; the track momentum values are limited as

$\frac{|p_1-p_2|}{|p_1+p_2|} < 0.15$  ( $< 0.2$  for  $E_{beam} < 955$  MeV), and the total energy deposition in the calorimeter is  $> 200$  MeV.

The criteria at SND and  $E_{beam} < 960$  MeV are the following (preliminary): exactly 3 tracks with a common vertex located in the beam pipe material, and no other tracks (proton is not registered). At  $E_{beam} \geq 960$  MeV two collinear central tracks in DC with large dE/dx are required, the total energy deposition in the calorimeter is  $> 650$  MeV, one of tracks should not have any associated calorimeter cluster.

The  $p\bar{p}$  cross sections ( $\sigma_{p\bar{p}}$ ) were obtained from the well known expression:

$$N = \varepsilon \delta \sigma_{p\bar{p}} \cdot L \quad (4)$$

where  $N$  - is the number of events,  $L$  is the integrated luminosity,  $\varepsilon$  is the detection efficiency, and  $\delta$  is the radiative correction. The systematic uncertainty is estimated to be 6% for CMD-3 and 7% for SND.

Fit of the  $\cos\theta$  distribution to extract  $\frac{G_E}{G_M}$  is also made for both experiments. The results are  $\frac{G_E}{G_M} = 1.49 \pm 0.23 \pm 0.3$  at CMD-3 ([8]) and  $\frac{G_E}{G_M} = 1.64 \pm 0.26$  at SND (preliminary result).

The cross section for the CMD-3 [8] and for the SND (preliminary) are shown at Fig.3 and at Fig.4.

Fig. 3. The CMD-3  $p\bar{p}$  cross section and angle distribution .

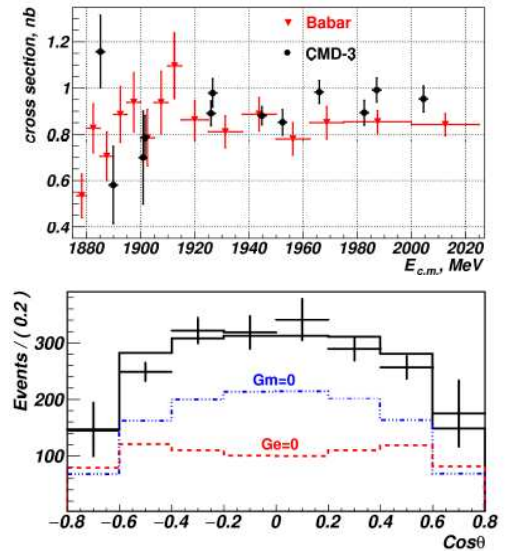
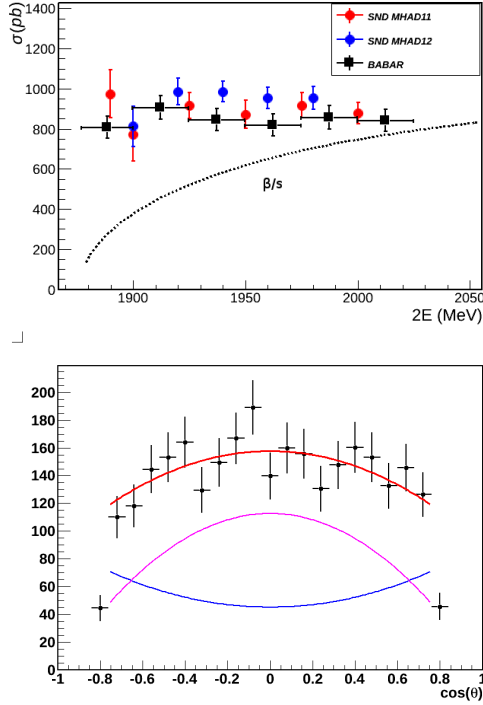
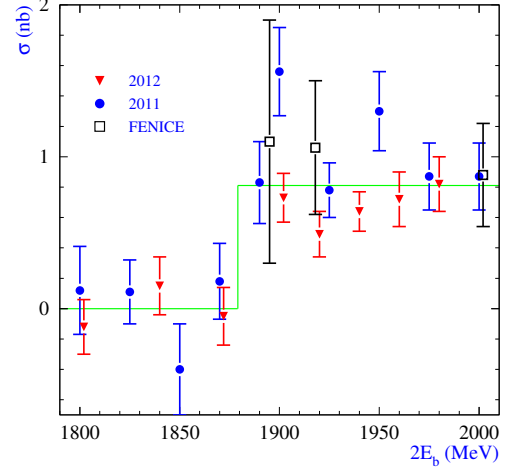


Fig. 4. The SND  $p\bar{p}$  cross section and angle distribution , preliminary results.


 Fig. 5. The SND  $n\bar{n}$  cross section.


## 4 Discussion

The  $e^+e^- \rightarrow p\bar{p}$  cross section is almost constant, through it is natural to expect its decrease as  $\beta/s = \frac{\sqrt{1-4M^2}}{s}$  when approaching the threshold (Fig.4). Both SND and CMD-3 results (Fig.6) confirm the Babar result, that  $\frac{G_E}{G_M}$  near threshold strongly differs from unity. This was somewhat unexpected, because of  $G_E = G_M$ .

 Fig. 6. The  $p$  EM form factors ratio .

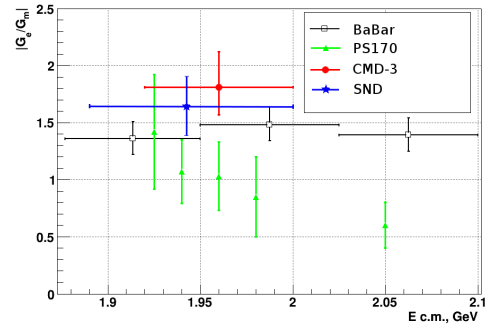
## 3 SND $n\bar{n}$ measurement

To select events from the  $e^+e^- \rightarrow n\bar{n}$  process all events that meet criteria for  $e^+e^- \rightarrow e^+e^-$  and  $e^+e^- \rightarrow 2\gamma$  are removed explicitly, cosmic background is suppressed with the muon system veto, at least two clusters in the EMC calorimeter are required in the event, other criteria utilize the energy:  $950\text{MeV} < E_{\text{EMC}} < 950\text{MeV}$ , and the total event momentum registered in calorimeter:  $P_{\text{EMC}} > 0.5 \cdot E_{\text{beam}}$ ,  $25^\circ < \theta_{P_{\text{EMC}}} < 155^\circ$ .

To extract the cross section ( $\sigma_{n\bar{n}}$ ) from the number of events ( $N$ ) the following expression taking into account cosmic background is used:

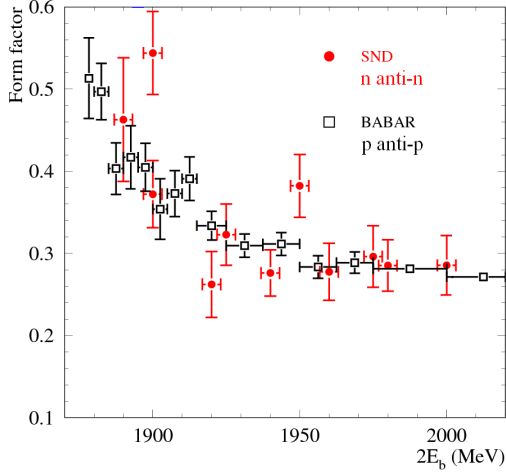
$$N = \sigma_{\text{TH}} \cdot L + \sigma_{p\bar{p},\text{VIS}} \cdot L + x \cdot T + \varepsilon \delta \sigma_{n\bar{n}} \cdot L$$

where  $\sigma_{p\bar{p},\text{VIS}}$  is a visible  $p\bar{p}$  cross section passed  $n\bar{n}$  selection criteria,  $\sigma_{\text{TH}}$  is a visible cross section of processes with smooth behavior near  $n\bar{n}$  pair production threshold,  $x$  is the visible cosmic events rate,  $T$  is the time of data taking for particular energy,  $L$  is the integrated luminosity,  $\varepsilon$  is the detection efficiency, and  $\delta$  is the radiative correction. The visible cosmic event rate is obtained with a common fit in all energy points and found to be  $(1.40 \pm 0.07) \cdot 10^{-3} \text{Hz}$ . For  $\sigma_{\text{TH}}$  its direct measurement below  $n\bar{n}$  threshold is used, but it is also estimated from possible physical background processes contributions and found to be in a good agreement. The obtained cross section separately for two seasons and early data from FENICE[7] are shown at Fig.5.



The  $e^+e^- \rightarrow n\bar{n}$  cross section is also constant (Fig.5) also and coincides within the errors with that for  $e^+e^- \rightarrow p\bar{p}$  (Fig.7). The  $\sigma_p = \sigma_n$  relation suggests that either isoscalar or isovector amplitude dominates in the  $e^+e^- \rightarrow n\bar{n}$  process near threshold. The pQCD asymptotics is  $\frac{\sigma_p}{\sigma_n} = 4$ .

Fig. 7. Nucleon effective form factor.

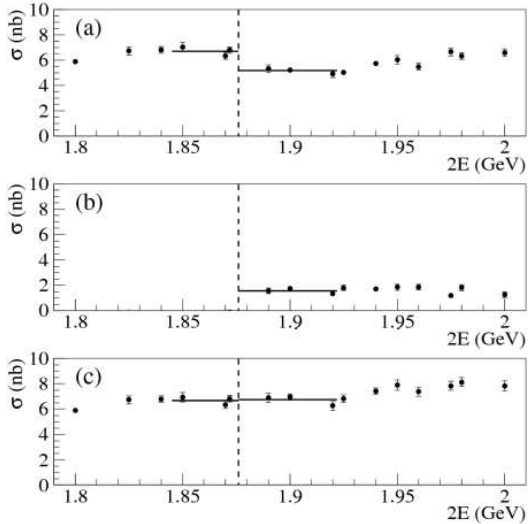


Possible explanations of this observation could be:

- sub-threshold resonance;
- final state interaction between nucleons.

The theoretical discussion of the phenomenon on the base of Paris nucleon-antinucleon optical potential [10] suggests that isoscalar channel dominance should lead to attraction while isovector to repulsion. However it is noted [11] that  $e^+e^- \rightarrow n\bar{n}$  threshold jump has almost equal value and opposite sign with isovector part of  $e^+e^- \rightarrow 3(\pi^+\pi^-)+2(\pi^+\pi^-\pi^0)$  processes (Fig.8). In other multipion channels any features compatible in magnitude are not observed near nucleon pair production threshold.

Fig. 8.  $e^+e^- \rightarrow n\bar{n}$  and isovector  $e^+e^- \rightarrow 6\pi$  jump compensation .



## References

- 1 D. E. Berkaev et al., JETP 113 (2011), 213.
- 2 M. N. Achasov et al., Nucl. Instrum. Methods Phys. Res., Sect. A 449, 125 (2000); *ibid.* 598, 31 (2009); V. M. Aulchenko et al.,

## 5 Conclusions and plans

Cross section of the  $e^+e^- \rightarrow p\bar{p}$  is measured independently with the CMD-3 detector and with the SND detector at VEPP-2000 collider, timelike effective electromagnetic form factor of proton, ratio of electric and magnetic form factors are extracted.

Cross section of the  $e^+e^- \rightarrow n\bar{n}$  is measured with the SND detector, timelike effective electromagnetic form factor of neutron, ratio of electric and magnetic form factors are extracted.

Results for both the neutron and the proton form factor near the pair production threshold agree well with previous measurements (Babar, FENICE), but raise some interpretation questions.

Future modernization of collider and both detectors would allow to improve these results. VEPP-2000 undergoes upgrade of electrons and positrons source which will allow to increase a luminosity by the order of magnitude. For the new runs the laser Compton backscattering method will be used for the beam energy measurement. Electronics upgrade of the SND detector will allow the time measurement in the calorimeter to better separate antineutron signal from the cosmic background. The new time of flight (TOF) system on the CMD-3 detector will also improve power of antineutrons selection.

## 6 Acknowledgments

This work is supported in part by the Russian Education and Science Ministry in the framework of the State order, by the Russian Foundation for Basic Research grants RFBR 15-02-03391 and scientific school grant 5320.2012.2.1460424-5. Part of this work related to the photon reconstruction algorithm and alignment in the SND electromagnetic calorimeter is supported by Russian Science Foundation (project N 14-50-00080).

- ibid.* 598, 102 (2009); A. Yu. Barnyakov et al., *ibid.* 598, 163 (2009); V. M. Aulchenko et al., *ibid.* 598, 340 (2009) .
- 3 V. M. Aulchenko et al., BUDKER-INP-2001-45. ; G. V. Fedotovich et al., Nucl. Phys. Proc. Suppl. 162 (2006), 332.

- 4 A. B. Arbuzov, T. V. Kopylova, JHEP 1204, 009 (2012); e-Print: arXiv:1111.4308 .
- 5 J. P. Lees et al. (BABAR Collaboration), Phys. Rev. D 88, 072009 (2013) .
- 6 G. Bardin et al. (PS170 Collaboration), Nucl. Phys. B411, 3 (1994).
- 7 A. Antonelli et al, (FENICE Collaboration), Nucl. Phys. B517, 3 (1998) .
- 8 R.R. Akhmetshin et al. (CMD-3 Collaboration), e-Print: arXiv:1507.08013
- 9 M.N. Achasov et al., Phys.Rev. D90 (2014) 11, 112007; e-Print: arXiv:1410.3188 [hep-ex]
- 10 V. F.Dmitriev, A.I.Milstein, S.G.Salnikov Phys.Atom.Nucl. 77 (2014) 1173
- 11 A.E. Obrazovsky, S.I. Serednyakov JETP Lett. 99 (2014) 363